Picosecond Spectroscopy Studies of the Intersystem Crossing of Aromatic Carbonyl and Nitro Compounds in Solution

Hiroyuki OHTANI, Takayoshi KOBAYASHI,† Kaoru SUZUKI, and Saburo NAGAKURA*

Institute for Solid State Physics, The University of Tokyo, Roppongi, Minato, Tokyo, 106

†*The Institute of Physical and Chemical Research, Wako, Saitama 351*

(Received July 16, 1979)

The build-up time constants of $T_n \leftarrow T_1$ transition bands were measured with 4-hydroxybenzophenone, Michler's ketone, 2-nitrofluorene, 1-nitropyrene, and 9-nitroanthracene in solution with the aid of picosecond spectroscopy. All the compounds exhibit fast build-up of the $T_n \leftarrow T_1$ absorption with the time constants smaller than 100 ps. The picosecond kinetics of these nonfluorescent compounds are interpreted in terms of the electronic structures of initial and final states relevant to radiationless transitions.

Aromatic carbonyl and nitro compounds are well known to be nonfluorescent.[1-3] Benzophenone exhibits strong phosphorescence, the quantum yield of the triplet formation being unity.[3] Therefore, the nonfluorescent property of benzophenone is caused by the fast S-T intersystem crossing. The quantum yields of the triplet formation are 0.63 and 0.83[4] for 1- and 2-nitronaphthalenes which are nonfluorescent and show weak phosphorescence, respectively.[2] Since the yield of fluorescence, $\Phi_F(=k_f/(k_f+k_{nr})$, $k_f=10^6$—$10^7\ s^{-1})$ is smaller than 10^{-4} for these molecules, the nonradiative rate constant, k_{nr}, is larger than $10^{10}\ s^{-1}$ and the nonradiative relaxation process occurs in the time scale of subnanosecond.

Nonradiative decay time constants of aromatic carbonyl compounds,[5-9] nitronaphthalene,[6] acridine,[10,11] and phenazine[10] have been measured so far by monitoring $T_n \leftarrow T_1$ absorption with picosecond time-resolved spectroscopy.

In a previous paper[7] we reported the intersystem crossing rate of anthrone and fluorenone. In anthrone the break-down of the El-Sayed rule was explained by the second order perturbation theory considering the vibronic interactions between appropriate states. In the present paper the nonradiative decay processes of excited singlet states have been studied for 4-hydroxybenzophenone, Michler's ketone (4,4'-bis(dimethylamino)benzophenone), 2-nitrofluorene, 1-nitropyrene, and 9-nitroanthracene.

Experimental

Picosecond Experiments. Figure 1 shows a picosecond time-resolved spectroscopy apparatus which is similar to the one described in the previous paper.[7] We used one OMA instead of two. The double-beam method[7,12] is effective for reducing deviations caused by the shot by shot change in spatial intensity distribution of the picosecond pulse. The frequency of a single pulse (694.3 nm, 30±3 ps pulse width, several giga watts) selected from a pulse train from a mode-locked ruby laser was doubled with a phase-matched ADP crystal. The frequency-doubled pulse (347.2 nm) was used for the excitation of samples through a pinhole (0.9 mm in diameter) of a sample cell holder. By passing the fundamental pulse through a phosphoric acid cell (20 mm in diameter, 100 mm in light path) a picosecond pulse of continuum light was generated. The pulse was divided into 14 pulses by an echelon with the time interval of 19.0 ps between the neighbouring pulses. These pulses were divided into two sets by a beam splitter.

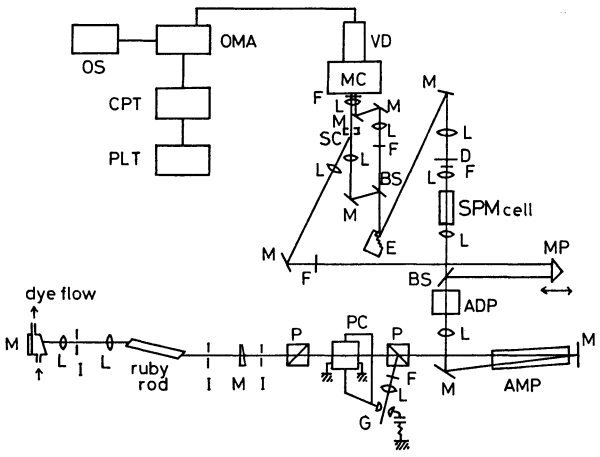

Fig. 1. The block diagram of the picosecond spectroscopy apparatus.
M: Mirror, L: lens, I: iris, P: polarizer, PC: Pockels cell, G: spark gap, BS: beam splitter, MP: movable prism, F: filter, SPM cell: self-phase modulation cell, D: diffuser, E: echelon, SC: sample cell, MC: monochromator, VD: vidicon, OMA: optical multichannel analyzer, OS: oscilloscope, CPT: computer, PLT: plotter.

One set passed through the Pyrex sample cell (light path 2.0 mm) and another set was used as reference. The observation wavelength was selected by a Shimadzu grating polychromator. Light intensities were detected by a vidicon head (PAR 1205 I) of an OMA (PAR 1205), digitized, and memorized in an OMA console (PAR 1205 A). The data were recorded in the digital cassette tapes and analyzed with a YHP 9825A desk-top computer. The results were printed out with the internal thermal printer of the computer or plotted with a YHP 9862A X-Y plotter.

Materials. 4-Hydroxybenzophenone (Tokyo Kasei), Michler's ketone (4,4'-bis(dimethylamino)benzophenone) (Tokyo Kasei), 2-nitrofluorene and 9-nitroanthracene (Aldrich) were purified by repeated recrystallizations and/or column chromatography. 1-Nitropyrene kindly supplied by Prof. T. Yamaoka, Chiba University was purified by repeated recrystallizations from ethanol. Ethanol (Wako, spectrograde) and benzene (Tokyo Kasei, UVIR grade) were used without further purification. Concentrations of samples were set in such ways that the absorbances at 337.1 nm were 1.0 in a 1 mm cell for nanosecond time-resolved spectroscopy experiments and those at 347.2 nm were at least 1.5 in a 1 mm cell for picosecond time-resolved spectroscopy experiments.

Results

Nanosecond Time-resolved Spectroscopy Experiments. Since the $T_n \leftarrow T_1$ spectra of 2-nitrofluorene, 9-nitroanthracene and Michler's ketone in benzene have never been reported, we measured their spectra with the nanosecond apparatus.[7] The strong absorption of Michler's ketone was observed between 420 nm and 600 nm in benzene solution. 2-Nitrofluorene exhibits strong absorption between 400 nm and 650 nm with a peak at 510—550 nm. The $T_n \leftarrow T_1$ absorption spectrum of 9-nitroanthracene resembles that of anthracene. All these transient absorption are assigned to $T_n \leftarrow T_1$ transitions, since the transient species are quenched by oxygen.

Picosecond Time-resolved Spectroscopy Experiments. Figures 2—6 show the time dependence of the $T_n \leftarrow T_1$ absorption intensity. Data of 7—14 shots are averaged for each point. Error bars in these figures represent standard deviations. The time constants were determined by the computer simulation on the assumptions described below. Before the measurement of the build-up of the $T_n \leftarrow T_1$ absorption of each sample we observed the build-up of the $S_n \leftarrow S_1$ absorption of coronene to determine the time resolution of the apparatus under the same monitoring wavelength and optical allignment. With the aid of formulas (1) and (2) we made computer simulation to determine the pulse width of the light source and the arrival time difference between the excitation pulse and the monitoring pulse train:

$$A(t) = -\log\left[\int_{-\infty}^{\infty} I(t-t')10^{-S(t')}\mathrm{d}t' \Big/ \int_{-\infty}^{\infty} I(t-t')\mathrm{d}t'\right] \quad (1)$$

$$S(t') = \Delta S \int_{-\infty}^{t'} I_{ex}(t''-t_0)\mathrm{d}t''$$

$$= \Delta S \int_{-\infty}^{t'} \frac{1}{\sqrt{\pi}G} e^{-(t''-t_0)^2/G^2}\mathrm{d}t'' \quad (2)$$

Here $A(t)$ is the absorbance for the $S_n \leftarrow S_1$ transition of coronene at time t, $I(t-t')$ is the monitoring pulse intensity at time t' which has the maximum at time t, ΔS is an experimentally determined parameter corresponding to the absorbance for the $S_n \leftarrow S_1$ transition of coronene at $t=\infty$, and $I_{ex}(t''-t_0)$ is the excitation pulse intensity at time t'' which has the maximum at time t_0. We assumed that excitation and monitoring pulses are gaussian and have the same pulse width (fwhm is $2 \ln G$). The time constant of the build-up of the $T_n \leftarrow T_1$ absorption (τ) and the contribution of $S_n \leftarrow S_1$ absorption (W) were obtained by the simulation of $A(t)$ to the observed curve by formulas (3) and (4),

$$A(t) = -\log\left[\int_{-\infty}^{\infty} I(t'-t)10^{-T(t')}\mathrm{d}t' \Big/ \int_{-\infty}^{\infty} I(t'-t)\mathrm{d}t'\right] \quad (3)$$

$$T(t') = \Delta A \int_{-\infty}^{t'} I_{ex}(t''-t_0)[W+(1-W)(1-e^{-(t-t'')/\tau})]\mathrm{d}t'' \quad (4)$$

where $T(t')$ is the transient absorption at time t' and consists of the $S_n \leftarrow S_1$ absorption and $T_n \leftarrow T_1$ absorption at the monitoring wavelength and ΔA is an experimentally determined parameter corresponding to the absorption for the transient absorption at $t=\infty$. The best-fit curve for each sample is shown in Figs. 2—6. The $T_n \leftarrow T_1$ build-up time constants thus determined are tabulated in Table 1. Error limits of

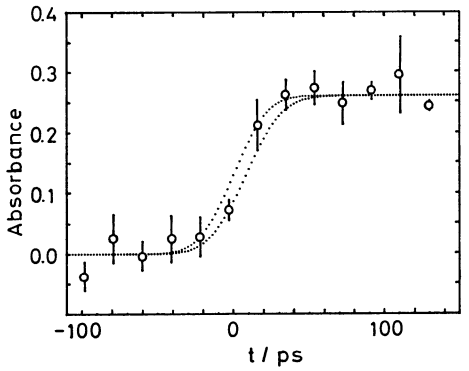

Fig. 2. Kinetics of $T_n \leftarrow T_1$ absorption at 550 nm for 4-hydroxybenzophenone in benzene. The time constants are 0 ps for •••• (upper) and 8 ps for •••• (lower).
The fraction of $S_n \leftarrow S_1$ absorption (W) is 0.0.

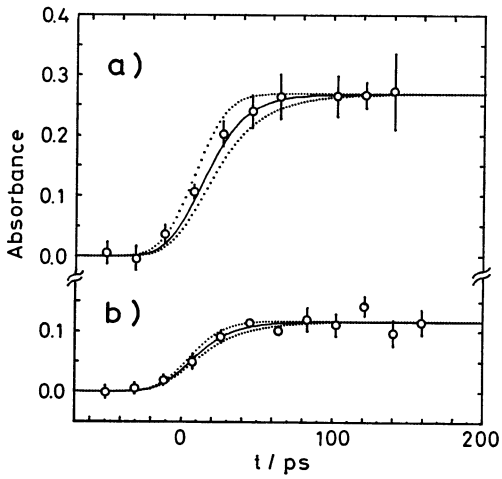

Fig. 3. Kinetics of $T_n \leftarrow T_1$ absorption at 550 nm for Michler's ketone: a) in benzene; b) in ethanol.
The time constants are 10 ps •••• (upper), 18 ps for —, and 26 ps for •••• (lower) in both a) and b).
The contribution of $S_n \leftarrow S_1$ absorption, is 0.0 for a) and 0.3 for b).

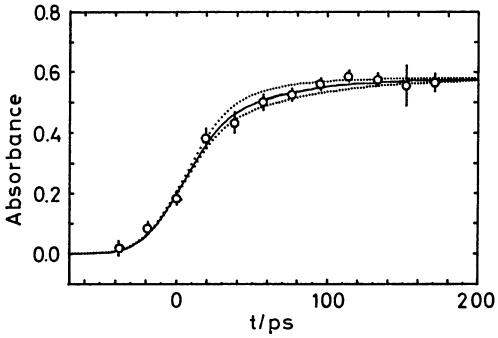

Fig. 4. Kinetics of $T_n \leftarrow T_1$ absorption at 520 nm for 2-nitrofluorene in benzene.
The time constants are 30 ps for •••• (upper), 45 ps for —, and 60 ps for •••• (lower), W being 0.6.

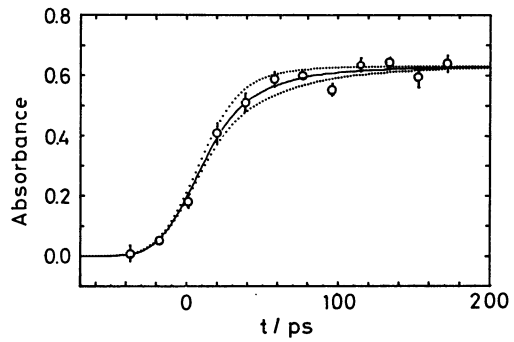

Fig. 5. Kinetics of $T_n \leftarrow T_1$ absorption at 520 nm for 1-nitropyrene in benzene.
The time constants are 20 ps for •••• (upper), 33 ps for —, and 46 ps for •••• (lower), W being 0.5.

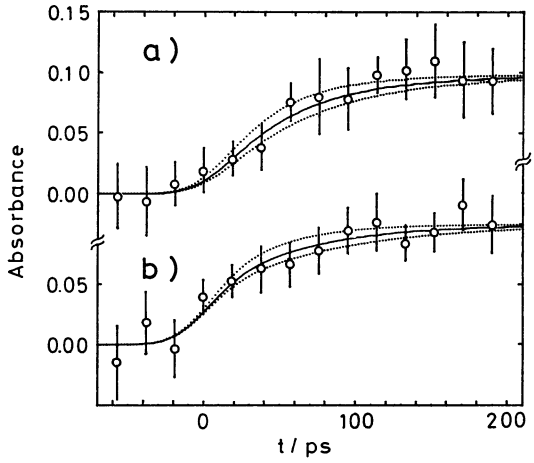

Fig. 6. Kinetics of $T_n \leftarrow T_1$ absorption for 9-nitroanthracene in benzene: a) observed at 450 nm where the $T_n \leftarrow T_1$ absorption is strong but the probing light intensity is reduced by the $S_1 \leftarrow S_0$ absorption tail: b) observed at 490 nm where the $T_n \leftarrow T_1$ absorption is weak the $S_1 \leftarrow S_0$ absorption intensity is negligibly small.
The time constants are 37 ps for •••• (upper), 50 ps for —, and 63 ps for •••• (lower) in a); 38 ps for •••• (upper), 58 ps for —, and 78 ps for •••• (lower) in b). The W value is 0.4 for both a) and b).

the time constants were determined in the following way. Simulation curves for the total absorbance of $T_n \leftarrow T_1$ and $S_n \leftarrow S_1$ absorptions were obtained with various build-up time constants of the triplet formation. The determined $\Delta\tau$ is the maximum of $\delta\tau$ which satisfies the following conditions; at least one of the two simulated curves with the time constants of $\tau+\delta\tau$ and $\tau-\delta\tau$ crosses all the error bars of absorbances at the respective steps of the echelon in the build-up part of the observed rising curves.

Discussion

The rate of the intersystem crossing depends on the matrix elements of the spin-orbit interaction between initial and final states. The selection rules for the radiationless transitions between electronic states with different spin-multiplicities were derived by El-Sayed.[13] The El-Sayed rule is applicable to the intersystem crossing process of many organic compounds. The break-down of this rule, however, has been observed for some cases: for example, benzophenone[14] and 9,10-diazaphenanthrene.[15] In the following we discuss the observed intersystem crossing rates in terms of the electronic structures of initial and final states relevant to the intersystem crossing.

Table 1. $T_n \leftarrow T_1$ build-up time constants at 347.2 nm excitation (room temperature)

Molecule	Solvent	λ_{obsd} / nm	τ [a] / ps	
			This work	Other authors
4-Hydroxy-benzophenone	Benzene	550	<8	
Michler's ketone	Benzene	550	18±8	
	Ethanol	550	18±8	
1-Nitronaphthalene	Benzene	533	—	12±5[b]
2-Nitronaphthalene	Benzene	533	—	10±2[b]
2-Nitrofluorene	Benzene	520	45±15	
1-Nitropyrene	Benzene	520	33±13	
9-Nitroanthracene	Benzene	450	50±13	
	Benzene	490	58±20	

a) τ is the $T_n \leftarrow T_1$ build-up time constant. b) λ_{ex} = 355 nm, λ_{obsd} = 533 nm.[6]

Aromatic Carbonyl Compounds. The intersystem crossing is a dominant deactivation process for benzophenone and 4-hydroxybenzophenone because its quantum yield, Φ_{ISC}, is unity and 0.9 for the former and the latter, respectively.[16] As for Michler's ketone, Φ_{ISC} is large in benzene (1.0) but small in ethanol (0.08).[17]

The $T_n \leftarrow T_1$ build-up time constant of benzophenone has been observed by several authors.[5,6,9] Recently, Hochstrasser and collaborators determined the value to be 12±2 ps in the benzene solution.[18] In the present study the $T_n \leftarrow T_1$ build-up time constant of 4-hydroxybenzophenone was found to be smaller than that of benzophenone, although the value was smaller than the time resolution of our apparatus. The energy level diagram of 4-hydroxybenzophenone is similar to that of benzophenone[19–23] and the lowest excited singlet state and the lowest triplet state have the n-π^* characters for both compounds. Therefore, 4-hydroxybenzophenone is another example deviating from the El-Sayed rule for the intersystem crossing rate. Its fast intersystem crossing may be explained, as in the cases of benzophenone and anthrone,[7] by the second order perturbation theory which considers vibronic couplings between the S_1 and S_2 states and also between the T_1 and T_2 states.[24,25]

The energy level diagram of Michler's ketone[26] in ethanol and in benzene are shown in Fig. 7; the diagram for the benzene solution is assumed to be the same as in hexane.[26] Since the yield of triplet formation is unity for Michler's ketone in benzene,[17] the observed time constant (18 ps) corresponds to the intersystem crossing rate constant. From the El-Sayed rule, we can expect the large spin-orbit coupling and the fast intersystem crossing for Michler's ketone in benzene,

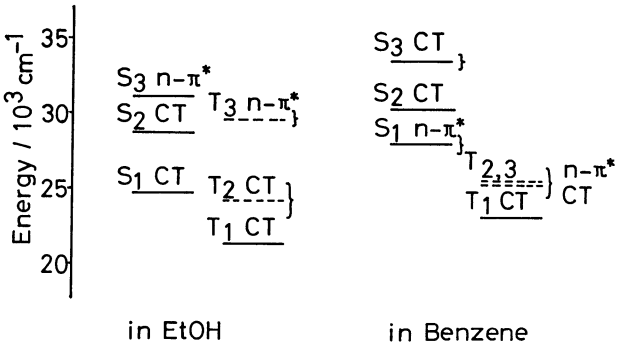

Fig. 7. Energy level diagrams of Michler's ketone in benzene and in ethanol.

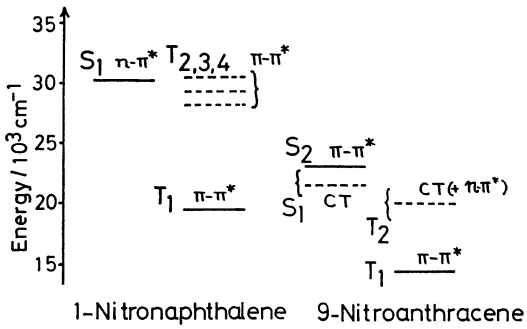

Fig. 8. Energy level diagrams of 1-nitronaphthalene and 9-nitroanthracene.
a) 1-Nitronaphthalene: S_1, determined from the absorption spectrum,[31] the triplet (π-π^*) states near S_1, estimated by the CNDO-CI calculation;[31] T_1 determined from the phosphorescence spectrum.[1,2]
b) 9-Nitroanthracene: S_1 and S_2, determined from the absorption spectrum.[32] The triplet state, determined from the $T \leftarrow S_0$ absorption spectrum.[33]
——: Experimentally determined level, ----: calculated level.

since the initial state is $S_1(n\text{-}\pi^*)$ the final state is T_2 (CT).

Concerning Michler's ketone in ethanol the yield of triplet formation is 0.08[17] and the quantum yield of the photochemical reaction is below 10^{-4}.[17] This means that for this case the internal conversion to the ground state (S_0) is a main decay process of the lowest excited singlet state (S_1). The time constant of the intersystem crossing (k_{ISC}^{-1}) and that of the internal conversion (k_{IC}^{-1}) were determined to be 225 ps and 19 ps, respectively, by the use of the observed rate constant, $\tau^{-1}(=k_{IC}+k_{ISC})$ and the yield of triplet formation, $\Phi_T(=0.08)$.[17] The time constant of the intersystem crossing in ethanol (225 ps) is greater than that for benzene solution (18 ps). This fact is understandable, since the initial and final states are both of CT character in the ethanol solution (Fig. 7).

The rapid $S_1 \rightarrow S_0$ internal conversion (19 ps) of Michler's ketone in ethanol may be interpreted in terms of the proton transfer; the hydrogen bond is formed between Michler's ketone and ethanol in the ground state and the equilibrium position of hydrogen is changed in the excited state. Recently the proton-induced enhancement of the intersystem crossing[27] and the fluorescence quenching by proton transfer have been reported.[28,29]

Aromatic Nitro Compounds. The quantum yields of triplet formation are high for aromatic nitro compounds: 0.63 for 1-nitronaphthalene,[4] 0.83 for 2-nitronaphthalene,[4] and 0.6 for 1-nitropyrene.[30] These compounds exhibit strong $T_n \leftarrow T_1$ absorption. Therefore, the intersystem crossing is the important decay process of their singlet states. In aromatic nitro compounds the position of the CT state among other electronic states determines the rate of the intersystem crossing. Figure 8 shows the energy level diagrams of 1-nitronaphthalene[1,2,31] and 9-nitroanthracene.[1,2,32,33] Anderson *et al.*[6] reported the $T_n \leftarrow T_1$ build-up time constants of 1- and 2-nitronaphthalenes. Time constants of 1-nitronaphthalene in benzene and in ethanol are 10 ps and 12 ps, respectively. Using the quantum yields of triplet formation the time constants of the intersystem crossing for 1- and 2-nitronaphthalenes were determined to be 15.9 ps and 14.5 ps, respectively. Mikula *et al.*[31] calculated transition energies of 1-nitronaphthalene and reported that two π-π^* states and an n-π^* state are located 26300—37700 cm^{-1} corresponding to absorption band. The initial state of the intersystem crossing is the ^{1}n-π^*[2] state and the final state is the $^3\pi$-π^* states nearby.[31] The effective intersystem crossing causes the rapid build-up of the $T_n \leftarrow T_1$ absorption.

The ionization potential of naphthalene is 8.15 eV[34] and the CT state of 1-nitronaphthalene lies in the higher energy region. The CT state of 9-nitroanthracene lies under the ^{1}n-π^* states because the ionization potential of anthracene (7.47 eV)[35] is smaller than that of naphthalene. Thus the initial state of the intersystem crossing of 9-nitroanthracene is S_1(CT) and its final state is ^{3}CT or $^3\pi$-π^*. Since the yield of triplet formation may be less than unity for 9-nitroanthracene, the time constant of the intersystem crossing, k_{ISC}^{-1} is larger than the $T_n \leftarrow T_1$ build-up time constant, 50 ps. This time constant is larger than that of 1-nitronaphthalene and is reasonable for the intersystem crossing from ^{1}CT to $^3\pi$-π^* or ^{3}CT.

2-Nitrofluorene and 1-nitropyrene may be assumed to be intermediate cases between 1-nitronaphthalene and 9-nitroanthracene, since the ionization potentials of fluorene and pyrene (7.93 eV[36] and 7.53 eV,[37] respectively) lie between those of naphthalene and anthracene. The observed $T_n \leftarrow T_1$ build-up time constants of 2-nitrofluorene and 1-nitropyrene fall in between those of 1-nitronaphthalene and 9-nitroanthracene.

The authors wish to thank Professor Tsuguo Yamaoka, Chiba University for his kind gift of 1-nitropyrene.

References

1) C. J. Seliskar, O. S. Khalil, and S. P. McGlynn, "Excited States," ed by E. C. Lim, Academic Press, New York (1974), p. 231.
2) O. S. Khalil, H. G. Bach, and S. P. McGlynn, *J. Mol. Spectrosc.*, **35**, 455 (1970).
3) A. A. Lamola and G. S. Hammond, *J. Chem. Phys.*,

43, 2129 (1965).
4) R. Hurley and A. C. Testa, *J. Am. Chem. Soc.*, **90**, 1949 (1968); R. Rusakowicz and A. C. Testa, *Spectrochim. Acta, Part A*, **27**, 787 (1971).
5) P. M. Rentzepis and C. J. Mitschele, *Anal. Chem.*, **42**, 20 (1970).
6) R. W. Anderson, Jr., R. M. Hochstrasser, H. Lutz, and G. W. Scott, *Chem. Phys. Lett.*, **28**, 153 (1974).
7) T. Kobayashi and S. Nagakura, *Chem. Phys. Lett.*, **43**, 429 (1976).
8) S. Hirayama and T. Kobayashi, *Chem. Phys. Lett.*, **52**, 55 (1977).
9) D. E. Damschen, C. D. Merritt, D. L. Perry, G. W. Scott, and L. D. Talley, *J. Phys. Chem.*, **82**, 2268 (1978).
10) Y. Hirata and I. Tanaka, *Chem. Phys.*, **25**, 381 (1977).
11) V. Sundstrom, P. M. Rentzepis, and E. C. Lim, *J. Chem. Phys.*, **66**, 4287 (1977); L. J. Noe, E. O. Degenkolb, and P. M. Rentzepis, *J. Chem. Phys.*, **68**, 4435 (1978).
12) T. L. Netzel and P. M. Rentzepis, *Chem. Phys. Lett.*, **29**, 337 (1974).
13) M. A. El-Sayed, *J. Chem. Phys.*, **38**, 2834 (1963); S. K. Lower and M. A. El-Sayed, *Chem. Rev.*, **66**, 199 (1966).
14) S. Dym and R. M. Hochstrasser, *J. Chem. Phys.*, **51**, 2458 (1969).
15) C. T. Lin and J. A. Stikeleather, *Chem. Phys. Lett.*, **38**, 561 (1976).
16) A. A. Lamola and L. J. Sharp, *J. Phys. Chem.*, **70**, 2634 (1966).
17) D. I. Schuster, M. D. Goldstein, and P. Bane, *J. Am. Chem. Soc.*, **99**, 187 (1977).
18) G. W. Scott, R. W. Anderson, Jr., R. M. Hochstrasser, and H. Lutz, *Bull. Am. Phys. Soc.*, **20**, 46 (1975).
19) R. M. Hochstrasser and J. E. Wessel, *Chem. Phys. Lett.*, **19**, 156 (1973).
20) W. L. Dilling, *J. Org. Chem.*, **31**, 1045 (1966).
21) P. J. Wagner, M. J. May, A. Haug, and D. R. Graber, *J. Am. Chem. Soc.*, **92**, 5269 (1970).
22) G. Porter and P. Suppan, *Trans. Faraday Soc.*, **61**, 1664 (1965).
23) D. R. Kearns and W. A. Case, *J. Am. Chem. Soc.*, **88**, 5087 (1966).
24) N. Kanamaru, *Sci. Papers I.P.C.R.*, **71**, 85 (1977).
25) N. Shimakura, Y. Fujimura, and T. Nakajima, *Chem. Phys.*, **19**, 155 (1977).
26) E. J. J. Groenen and W. N. Koelman, *J. Chem. Soc., Faraday Trans. 2*, **74**, 58 (1978); *ibid.*, **74**, 69 (1978).
27) H. Shizuka, Y. Ishii, and T. Morita, *Chem. Phys. Lett.*, **51**, 40 (1977).
28) K. Tsutsumi and H. Shizuka, *Chem. Phys. Lett.*, **52**, 485 (1977).
29) M. A. El-Bayoumi, P. Avouris, and W. R. Ware, *J. Chem. Phys.*, **62**, 2499 (1975).
30) R. Scheerer and A. Henglein, *Ber. Bunsenges. Phys. Chem.*, **81**, 1234 (1977).
31) J. J. Mikula, R. W. Anderson, L. E. Harris, and E. W. Stuebing, *J. Mol. Spectrosc.*, **42**, 350 (1972).
32) L. Skulski and J. M. Kanabus, *Bull. Acad. Pol. Sci. Ser. Sci. Chim.*, **17**, 311 (1969).
33) J. B. Birks, "Photophysics of Aromatic Molecules," Willey-Interscience, New York (1970), p. 268.
34) F. Brogli, E. Heilbronner, and T. Kobayashi, *Helv. Chim. Acta*, **55**, 274 (1972).
35) R. Boschi, J. N. Murrell, and W. Schmidt, *Discuss. Faraday Soc.*, **54**, 116 (1972).
36) J. P. Maier and D. W. Turner, *Discuss. Faraday Soc.*, **54**, 149 (1972).
37) E. S. Pysh and N. C. Yang, *J. Am. Chem. Soc.*, **85**, 2124 (1963).